Modelling helical screw piles in clay using a transparent soil

C.C.Hird & S.A. Stanier
Department of Civil and Structural Engineering, University of Sheffield, Mappin Street, Sheffield, S1 3JD, UK

ABSTRACT: A transparent synthetic soil consisting of fumed silica particles and a pore fluid with matched refractive index has been used to represent clay in a physical model of the installation and undrained load-deflection performance of helical screw piles in a deep installation condition. A digital camera captures images during installation and load-deflection testing, allowing the use of particle image velocimetry (PIV) techniques to compute displacement fields around the piles. This experimental method is being used to assess the effect of the helical plate spacing ratio on the failure mode and load deflection performance of single and multi-helical plate screw piles loaded in tension and compression, at a constant strain rate. Initial results are presented indicating significantly differing behaviour with respect to the configuration of the helical screw pile. The precision of the PIV output is significantly better than in previous analyses conducted using transparent soils in similar non-intrusive modelling scenarios.

1 INTRODUCTION

Helical screw piles typically consist of a tubular or solid steel shaft onto which regularly spaced helical plates of up to 0.4 m diameter are welded. All the plates are of the same pitch so that minimum disturbance is caused to the soil during installation. These piles are suitable for a wide range of applications including: marine anchors and pier supports, temporary structure supports, support for road and rail signage and foundations for oil and gas pipelines.

The benefits of helical screw piles over displacement piles or continuous flight auger piles are the minimal disturbance caused by installation, their ease of removal and re-use, and their similar tensile and compressive load-deflection behaviour.

Research into the behaviour of helical screw piles founded in clay (Rao et al. 1991, Rao & Prasad 1993, Rao et al. 1993) has focused on multi-helix screw piles loaded in both compression and tension with varying embedment ratio (depth/diameter, H/D), measured from the soil surface to the centre of the helical plate and helical plate spacing ratio (spacing/diameter, s/D), measured from helical plate centre to centre. It was found that characteristic deep installation behaviour required $H/D \geq 4$. It was also found that the number of helical plates over a fixed length of shaft, the active length, had a significant effect on the ultimate capacity and stiffness response of the pile. A smaller s/D ratio led to a stiffer response and greater ultimate capacity. Photographic evidence suggested that for small s/D ratios soil between the helical plates was constrained to fail with a cylindrical failure surface between the plates, whereas this was not apparent for large s/D ratios. The above authors proposed that a maximum s/D of 1.5 be employed to ensure optimum performance and presented a simple estimation of capacity, accounting for varying s/D, which assumed a cylindrical failure surface between helical plates.

Physical modelling involving the use of transparent synthetic clay, laser aided tomography, digital imaging and particle image velocimetry (PIV) is currently being undertaken to investigate more fully the differences of deep helical screw pile behaviour caused by varying the s/D ratio and to assess the validity of assuming a cylindrical failure surface between helical plates in design. The paper outlines the modelling techniques and reports some initial results.

2 DEVELOPMENT OF TRANSPARENT CLAY

2.1 *Amorphous Silica Transparent Clay*

Transparent synthetic clay soil was originally developed using aggregated particles of precipitated amorphous silica and a blend of paraffinic solvent and mineral oil as a pore fluid with a matched refractive index (RI) (Iskander et al. 1994, 2002). This has been used to assist the study of deformations be-

neath pad footings (Liu et al. 2002), flow in prefabricated vertical drains (Welker et al. 1999) and, more recently, displacements caused by the installation of continuous flight augers (Hird et al. 2008). However, the soil is not perfectly transparent and models suffer from a degradation of transparency with increasing size. Hird et al. (2008) were limited to a maximum distance from the edge of the model to the plane of interest of 50 mm.

A similar material was developed (Gill & Lehane, 2001) using fumed silica and a similar pore fluid. This has been used to investigate penetrometer installation into clay and, subsequently, the deformation of vibro stone columns under load in a large cylindrical chamber (McKelvey et al. 2004). The scale of these latter experiments is far in excess of those conducted using the precipitated amorphous silica, implying superior post-consolidation transparency.

2.2 *Transparency Assessment*

The primary advantage of a transparent synthetic soil model is that, by utilizing a laser light sheet to highlight a plane of interest within the model, displacements of the soil can be observed non-intrusively and recorded using a digital camera. PIV analysis can then be conducted on the digital data. It should be noted that, to give the transparent soil sufficient texture for successful PIV, it may be necessary to add a small proportion of reflective particles which unfortunately reduces the transparency.

At the start of the current research on the behaviour of deep helical screw piles, the transparencies of soils made with the precipitated and fumed silica were compared. Transparent clay slurry was created by mixing the silica with the appropriate pore fluid and de-airing the mixture under a vacuum. The slurry was then dispensed into a Perspex enclosure with plan dimensions of 150 mm x 50 mm. A test card printed with random characters in various sizes of Times New Roman font was viewed horizontally through 150 mm of slurry and the minimum font size that could be read was determined.

Blends of technical white oil and paraffin oil were used as pore fluids. The pore fluid constituents were selected such that their RIs bracketed the RI of the silica and their ratios were systematically varied to determine the optimum values. At the optimum ratio, the minimum readable font sizes were point 3 and point 2 for the precipitated and fumed silica soils respectively.

As the transparency of the synthetic soil reduces during consolidation, it was important to assess the transparency of the material in its consolidated state. The effect of seeding the soil with reflective particles (as described below) had also to be taken into account. Samples of the two materials were thus consolidated under a vertical stress of 100 kPa in an aluminium enclosure with Perspex viewing windows and plan dimensions of 200 mm x 200 mm. Consolidation was conducted in stages using a pneumatic cylinder and square piston with drainage through porous plastic filters at the top and bottom of the sample. A 12 mm diameter cylindrical pile was installed into the centre of each sample and a laser light sheet used to highlight an axisymmetric plane within the model. This allowed the visibility of the pile, when viewed through about 100 mm of consolidated soil, to be assessed, Figure 1. In Figure 1a, the pile in precipitated silica soil is barely visible and scarcely any reflective particles can be seen. In Figure 1b, the improvement in fumed silica soil is very clear.

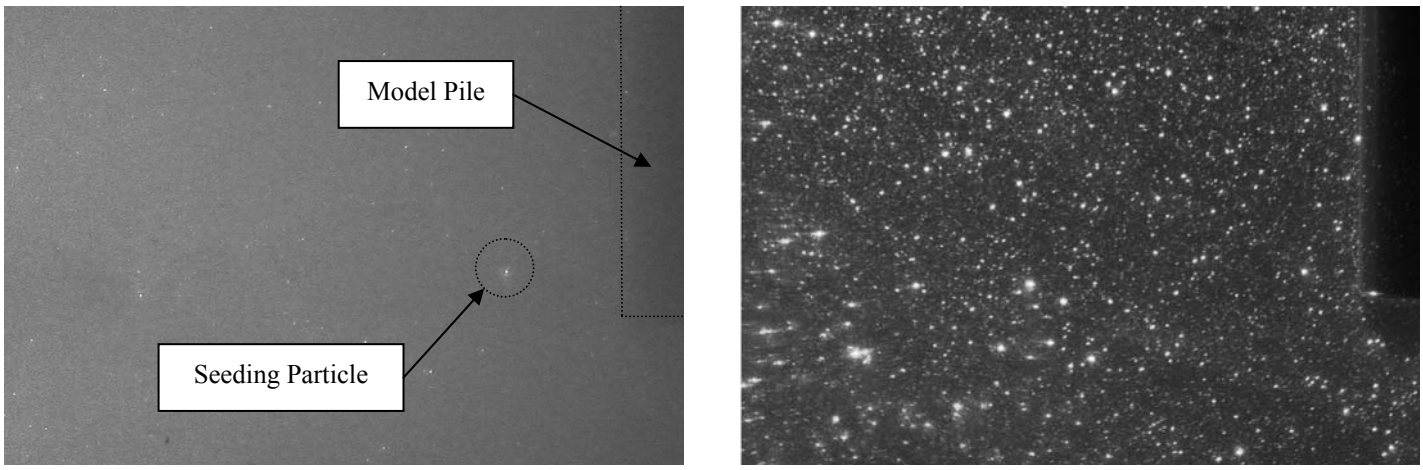

Figure 1. Comparison of visibility of 6 mm radius straight pile when viewed through 100 mm depth of precipitated silica soil (a) and fumed silica soil (b).

The superior transparency of fumed silica, as opposed to precipitated silica, in the synthetic soil has allowed the use of an enclosure twice the size of that previously utilized in continuous flight auger studies by Hird et al. (2008).

2.3 *Fumed Silica Transparent Clay Properties*

The physical properties of this fumed silica soil are broadly similar to those of natural clays, although the average compression index C_c of 10.5 and swelling index C_s of 0.86 are unnaturally high. This is attributed to the existence and breakdown of very fine particle aggregates. The average coefficient of consolidation C_v, measured during 50-100 kPa one-dimensional consolidation stages, was 3.93 m^2/year, while the indirectly measured permeability was around $4x10^{-9}$ m/s under the same stress increment and the vane shear strength in the models was about 16.5 kPa on average. Thus the soil represents soft highly compressible clay similar to that used previously (Gill & Lehane, 2001; McKelvey et al. 2004).

3 EXPERIMENTAL METHOD

3.1 *Model Formation*

Fumed silica powder is added to matched RI pore fluid in a ratio of 6:94 by mass. The soil required to fill the test chamber is mixed in two batches and reflective particles are seeded into one of them. The seeding particles consist of mica flakes coated with titanium oxide and have a size range of 10-60 μm. These particles are only seeded into the rear portion of the model so that the soil through which digital images are captured retains the optimum transparency (see Figure 3).

The soil slurries are de-aired under vacuum and poured with the aid of a split-mold into the aforementioned aluminium test enclosure and consolidated in stages to a maximum vertical stress of 100 kPa. After the gradual release of pressure, the final sample height is about 220 mm. In similar model testing, reported by Hird et al. (2008), a suction was applied at the base to generate an effective vertical stress at the soil surface. However, in this research no suction is applied. The main reason for this is the prevention of air ingress into the model from the surface as the piles are installed. Any ingress of air greatly impairs transparency and is now avoided by allowing a small depth (10 mm) of pore fluid to be present above the surface. A drawback of this procedure is that, while the undrained shear strength can be measured, the effective stresses in the model are unknown.

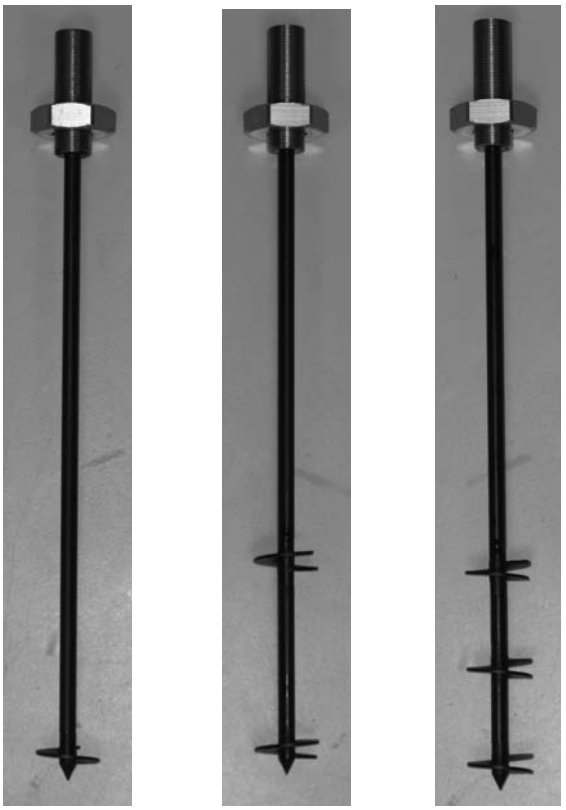

Figure 2. Helical screw pile assembled configurations: single helix pile (a), double helix pile where s/D=3.0 (b) and triple helix pile where s/D=1.5 (c).

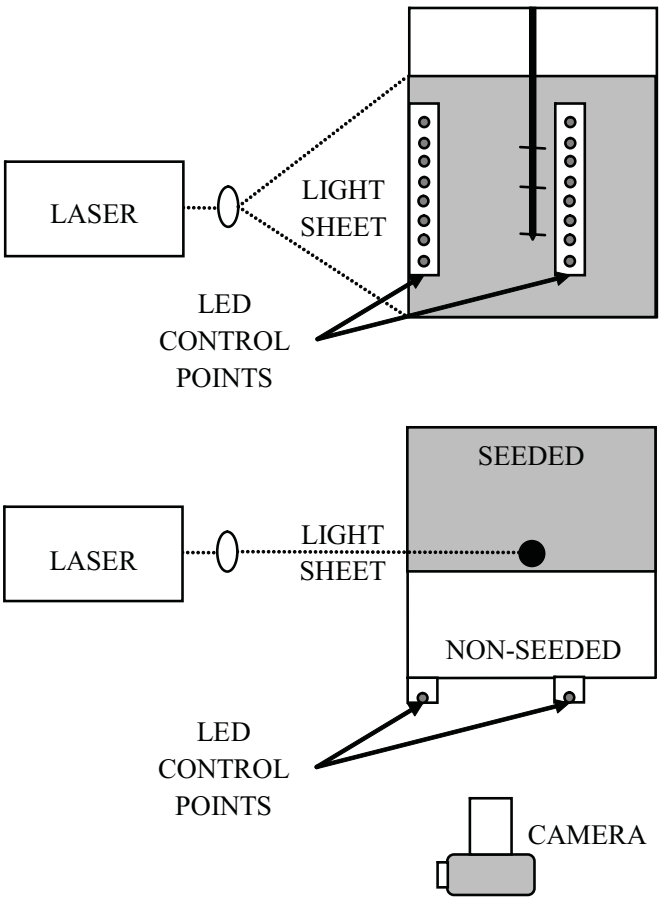

Figure 3. Experimental apparatus: schematic of camera view (a) and plan view (b).

3.2 *Model Helical Screw Piles*

The model helical screw piles consist of 20 mm diameter helices machined from billet aluminium with 5 mm pitch and 1mm plate thickness, connected by 5 mm diameter stainless steel shafts. The shaft lengths have been designed to allow the construction of the assembled configurations shown in Figure 2. The s/D ratio can be either 1.5 or 3. The pile components are painted black to minimise reflection of the laser light.

3.3 *Test Apparatus*

The test apparatus is illustrated schematically in Figure 3. Stepper motors with electronic control via the digital input/output channels of a data acquisition device (DAQ) are used to install the helical screw pile at a constant screw rate such that for every full rotation the pile advances axially by its flight pitch. A 450 mm draw-wire linear variable displacement transducer (LVDT) is used to monitor and halt installation of the pile when the required installation depth is achieved. A 1 watt argon ion laser is used to generate a laser beam which is shaped by a prismatic beam shaper into a light sheet of approximately uniform intensity over the height of the soil. This light sheet is aligned with the centreline of the pile allowing the observation of internal soil deformations during testing. A 250 N tension-compression load cell is used to measure the axial test load applied by the pile-driving rig to the model pile, and a 25 mm LVDT is used to record the axial displacement. Load-deflection data are recorded by the DAQ using an interface developed in LabVIEW.

3.4 *Test Procedure*

Pile installation and load-deflection testing are carried out at an axial displacement rate of 0.2 mm/s, chosen to ensure that sufficient digital image data could be recorded. Drainage during the load testing is judged to be minimal, based on the Lehane et al. (2008) relationship for estimating drainage beneath circular footings founded on clay. Applying strictly to surface loading, this should be conservative (overestimate drainage) if applied to footings at depth.

The model pile is installed to a depth of 7D or 140 mm ensuring that, for a multi-helix pile, the minimum embedment depth of any helical plate is 4D. After installation the pile is restrained, both axially and rotationally, for a period of 24 hours before load-deflection testing is conducted to allow excess pore pressures around the pile to dissipate.

Load-deflection testing is conducted whilst recording digital images using a Pentax K10-D SLR camera at rate of 3 frames/second, aligned such that half of the sample and two panels of light emitting diode (LED) control points are recorded. The control points are used during data processing to remove the effect of camera movement from the displacement data. Typically around 300 images are recorded during an axial pile displacement up to 20 mm.

3.5 *Data Processing*

The digital images are analysed using PIV processes, developed for geotechnical modelling by White et al. (2003), to derive pixel displacements of a mesh of target patches. These displacements are then corrected for radial and tangential lens distortion, camera pose and scaling using the methodologies outlined by Heikkilä & Silven (1997). Due to the improved clarity of the fumed silica compared with that of the precipitated silica (Figure 1), the precision of the PIV displacement measurements is significantly better than achieved previously in similar experiments (Hird et al. 2008). This is demonstrated in Figure 4 which shows the precision achieved as a function of patch size when an image of the fumed or precipitated silica soil was artificially displaced by an arbitrary number of pixels. Movement was tracked more precisely in the fumed silica despite the greater thickness of soil through which the illuminated plane was photographed, 100 mm rather than 50 mm. An upper bound relation suggested by White et al. (2003) is also shown for comparison.

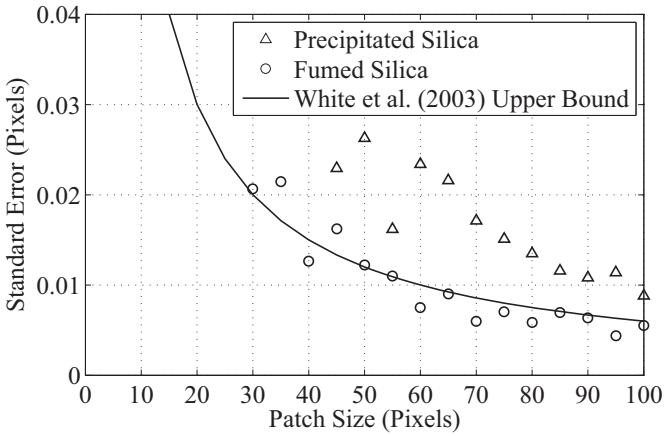

Figure 4. PIV precision for precipitated silica soil (a) and fumed silica soil (b).

4 INITIAL RESULTS

Results are presented here from two tests: a single helix screw pile compression test and a triple helix screw pile (s/D = 1.5) compression test. Figures 5 and 6 present plots of the soil displacements at a pile displacement of 2 mm (points marked in Figure 7 showing the load-deflection response) in vector, horizontal contour and vertical contour form. Negative displacements indicate movement away from the

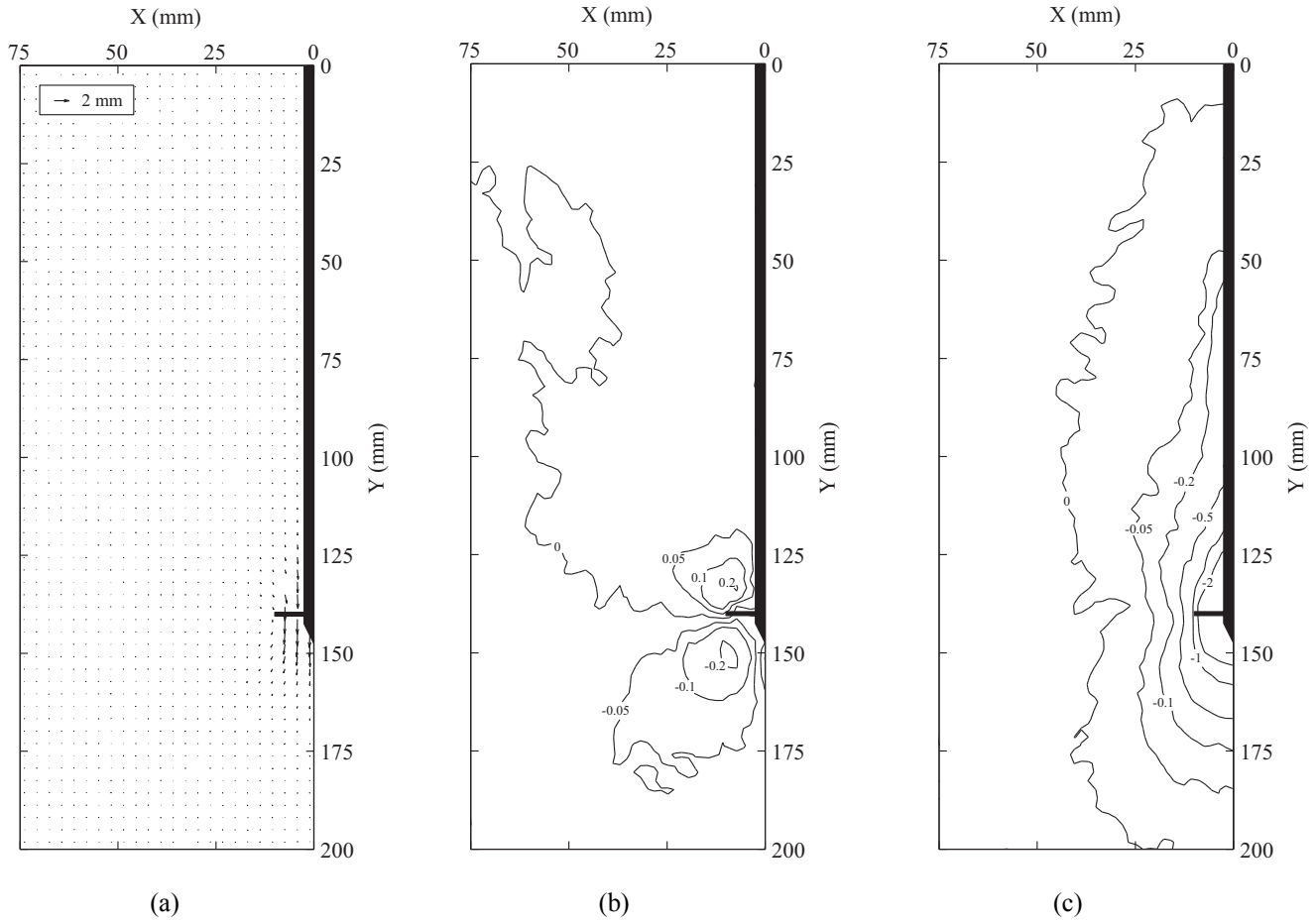

Figure 5. Vector (a), horizontal contour (b) and vertical contour (c) plots of the displacement fields caused by an axial displacement of 2.0 mm for a single helix screw pile with displacements in mm.

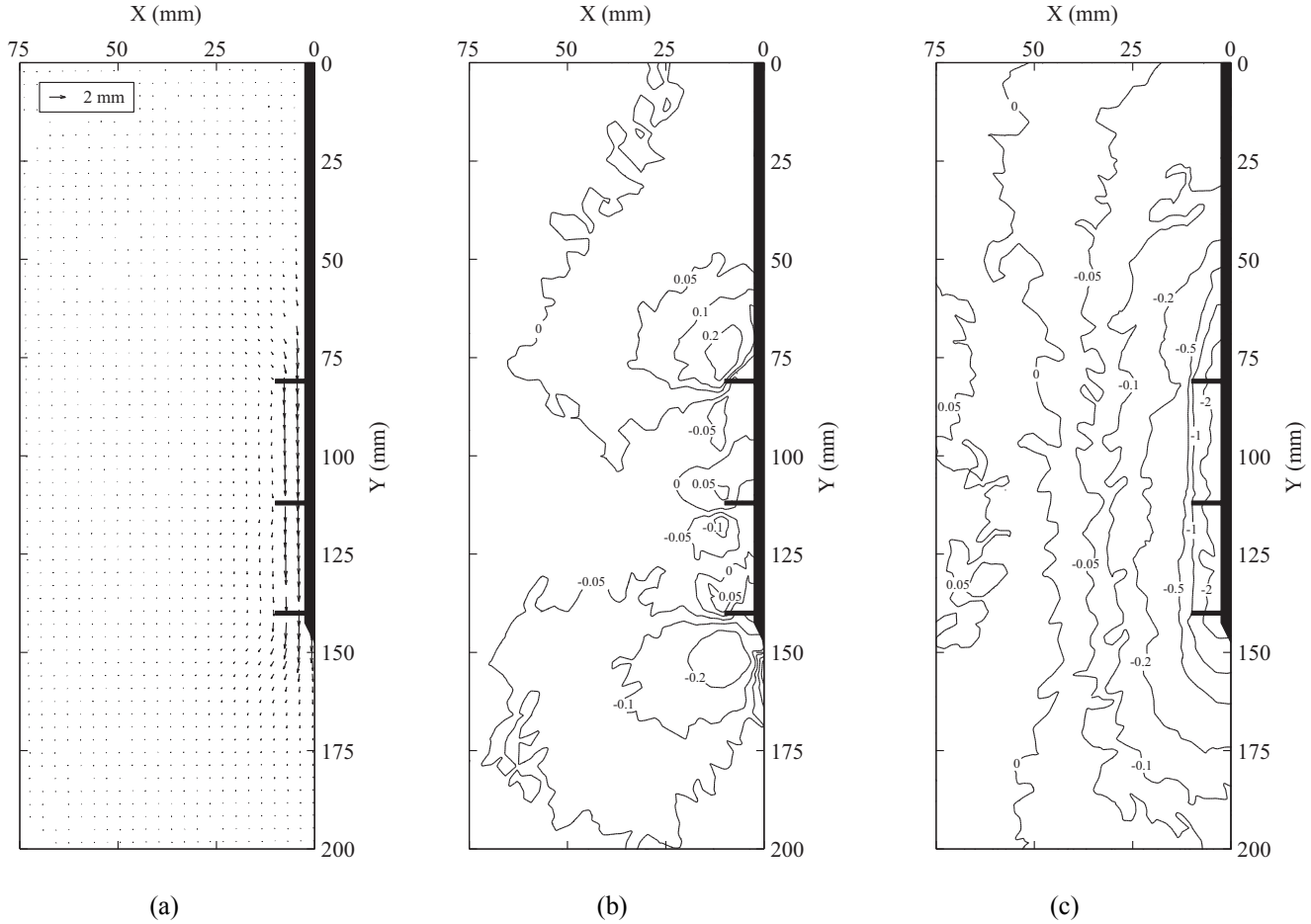

Figure 6. Vector (a), horizontal contour (b) and vertical contour (c) plots of the displacement fields caused by an axial displacement of 2.0 mm for a triple helix screw pile with displacements in mm.

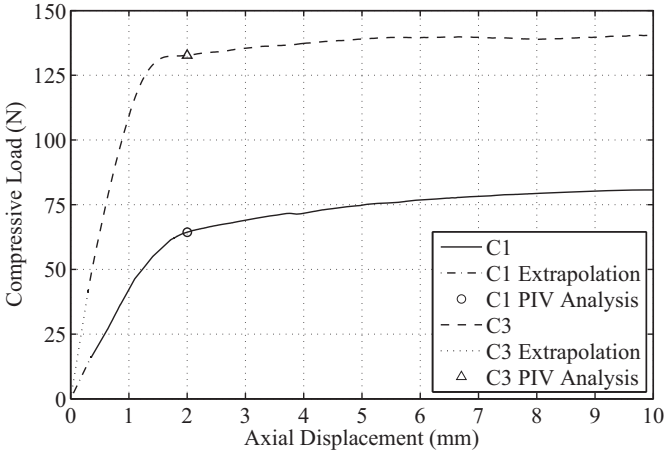

Figure 7. Load-deflection response of the two helical screw pile configurations.

pile in the horizontal contour plots and downward movement in the vertical contour plots.

The load-deflection responses in Figure 7 clearly show, as would be expected, that the triple helix screw pile (C3) exhibits increased stiffness and ultimate capacity compared to the single helix pile (C1). It should be noted that the measured load-deflection data does not start at the origin of the graph due to the presence of residual stress acting on the base of the pile after installation. This is caused by compression of soil below the pile base, even though it is being screwed in. The initial measured gradient of the load-deflection response has been used to extrapolate it back to the origin.

The single helix screw pile results show inward lateral movement above the helical plate and outward lateral movement below it (Figure 5b), and a small bulb of soil moving down with the plate (Figure 5c). For the triple helix screw pile, inward lateral movement occurs above the top helical plate and outward lateral movement below the bottom plate but between the plates there is relatively little horizontal movement (Figure 6b). Soil between the plates is largely carried down by the pile (Figure 6c). Therefore, soil is confined between the plates and, although a cylindrical failure surface is not yet fully developed over the active length, a shear band is forming. This suggests that the proposed failure mechanism of Rao et al. (1993) is likely to be valid when s/D=1.5 at large axial displacements.

5 CONCLUSIONS

Previously used modelling techniques (Hird at al. 2008) have been improved by switching from precipitated silica to fumed silica as the solid constituent of synthetic transparent clay in combination with a new pore fluid. The resulting improved transparency has allowed the use of larger models and given improved precision of displacement measurements. There is potential for this transparent material and the modelling techniques outlined in this paper to be used to investigate problems involving complex non-planar geometries or installation processes.

Initial results from an investigation of helical screw pile behaviour have been reported. A triple helical plate pile with a helical plate spacing ratio (s/D) of 1.5 had a higher capacity and stiffer compressive load-deflection response than a single helical plate pile. Soil was confined within the space between the plates on the triple plate pile such that a cylindrical failure surface formed. Research is ongoing into the effects of differing s/D ratios and active lengths on the tensile and compressive responses of helical screw piles in clay.

6 REFERENCES

Gill, D. & Lehane, B. 2001. An optical technique for investigating soil displacement patterns. *Geotechnical Testing Journal* 24(3): 324-329.

Heikkilä, J. & Silvén, O. 1997. A four-step camera calibration procedure with implicit image correction. *Proceedings of the 1997 Conference on Computer Vision and Pattern Recognition* pp. 1106–1112.

Hird, C., Ni, Q. & Guymer, I. 2008. Physical modelling of displacements around continuous augers in clay. *Proc. 2nd British Geotechnical Association International Conference on Foundations* 1: 565-574.

Iskander, M., Lai, J., Oswald, C. & Mannheimer, R. 1994. Development of a transparent material to model the geotechnical properties of soils. *Geotechnical Testing Journal* 17(4): 425-433.

Iskander, M., Liu, J. & Sadek, S. 2002. Transparent amorphous silica to model clay. *Journal of Geotechnical and Geoenvironmental Engineering* 128(3): 262-273.

Lehane, B., Gaudin, C., Richards, D. & Rattley, M. 2008. Rate effects on the vertical uplift capacity of footings founded in clay. *Géotechnique* 58(1): 13-21.

Liu, J., Iskander, M. & Sadek, S. 2002. Optical measurement of deformation under foundations using a transparent soil model. *Physical Modelling in Geotechnics: ICPMG 2002* pp. 155-159.

McKelvey, D., Sivakumar, V., Bell, A. & Graham, J. 2004. Modelling vibrated stone columns in soft clay. Proc. Institution of Civil Engineers: *Geotechnical Engineering* 3: 137-149.

Rao, S. & Prasad, Y. 1993. Estimation of uplift capacity of helical anchors in clays. *Journal of Geotechnical Engineering* 119(2): 352-357.

Rao, S., Prasad, Y. & Shetty, M. 1991. The behaviour of model screw piles in cohesive soils. *Soil and Foundations* 31(2): 35-50.

Rao, S., Prasad, Y. & Veeresh, C. 1993. Behaviour of embedded model screw anchors in soft clays. *Géotechnique* 43(4): 605-614.

Welker, A., Bowders, J. & Gilbert, R. 1999. Applied research using a transparent material with hydraulic properties similar to soil. *Geotechnical Testing Journal* 22: 266-270.

White, D., Take, W. & Bolton, M. 2003. Soil deformation measurement using Particle Image Velocimetry (PIV) and photogrammetry. *Géotechnique* 53(7): 619-631.